CRYSTAL GROWTH & DESIGN

Article

pubs.acs.org/crystal

Bistable and Porous Metal–Organic Frameworks with Charge-Neutral acs Net Based on Heterometallic $M_3O(CO_2)_6$ Building Blocks

Keunil Hong,[†] Woojeong Bak,[†] Dohyun Moon,*[,‡] and Hyungphil Chun*[,†]

[†]Department of Applied Chemistry, College of Science and Technology, Hanyang University, 55 Hanyangdaehak-ro, Ansan 426-791, Republic of Korea

[‡]Beamline Division, Pohang Accelerator Laboratory, Pohang, Kyungbuk 790-784, Republic of Korea

Supporting Information

ABSTRACT: A Co(II)–Ti(IV) heterometallic approach is successfully adopted to synthesize charge-neutral metal–organic frameworks based on oxo-centered trinuclear cluster and linear dicarboxylate linkers. Unlike their homonuclear predecessors, the cobalt–titanium–organic frameworks not only display a permanent porosity but also show an irreversible phase transition between two stable forms as unambiguously characterized by single-crystal and powder X-ray diffraction studies.

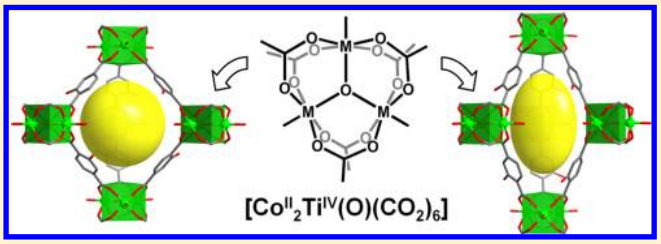

INTRODUCTION

Coordination polymers or metal–organic frameworks (MOFs) are one of the most intensely studied materials in the past decade, and find potential applications in such areas as separation, storage, catalysis, delivery, and others.[1] The unparalleled advantages of MOFs over other classes of porous materials include the facile synthesis in highly crystalline forms and vast diversities of frameworks and their components.

One of methods that would further enrich the structural diversities of MOFs is a heterometallic approach in the synthesis of new frameworks. Compared to conventional homonuclear systems, heterometallic MOFs are advantageous in introducing functional sites for catalysis or gas adsorption.[2] In a somewhat different perspective, we have recently shown that a partial inclusion of high-valent metal ions, such as Ti(IV), in porous Zn(II)-carboxylate MOFs may improve the long-term stability of evacuated solids in ambient air.[3] While attempting to generalize this approach, we discovered that the combination of Co(II)–Ti(IV) with simple dicarboxylate leads the formation of well-known trinuclear building blocks which in turn form open frameworks with intriguing dynamic properties (Scheme 1). Here we report the synthesis, crystal structures, gas sorption and highly unusual phase transition of cobalt–titanium–organic frameworks (CTOFs).

EXPERIMENTAL SECTION

Materials and Methods. All the reagents and solvents were commercially available and used as received. DSC-TGA data were obtained on a SCINCO S-1000 instrument with a heating rate of 5 °C/min in air (Supporting Information (SI) Figure S1). IR data were recorded on KBr pellets using a Varian FTS 1000 instrument (SI Figure S2).

CTOF-1. To a solution containing $Co(NO_3)_2{\cdot}6H_2O$ (70.0 mg, 0.24 mmol) in DMF (1.30 mL) added were 2-hydroxyterephthalic acid (54.6 mg, 0.30 mmol) and $TiCl_4(thf)_2$ (20.0 mg, 0.06 mmol). After it was stirred for about 30 min, the greenish solution was charged into a glass tube which was then flame-sealed and heated to 150 °C for 55 h. The tube was cut open (*be careful for a sudden release of pressure*) to collect the product as a mixture of double-pointed hexagonal blocks (CTOF-1w) and very small hexagonal plates (CTOF-1e) (~8:2). The as-synthesized crystals were soaked in CS_2 for several days and dried under vacuum overnight (26 mg, 60%). When the initial mixture was heated to 70 °C for 12 h, 90 °C for 24 h, and then to 115 °C for 72 h, only the CTOF-1w form is obtained with a slightly lower yield. Calcd for $Co_2Ti(O)(hbdc)_3{\cdot}5H_2O$: C, 35.49; H, 2.73; N, 0.00; Co, 14.51; Ti, 5.89. Found: C, 35.30; H, 2.26; N, 0.00; Co, 14.23; Ti, 5.68%.

Scheme 1. Secondary Building Unit and Organic Linkers in the Title Compounds

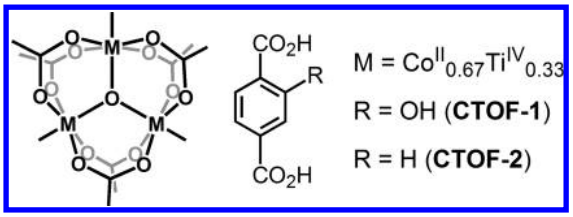

CTOF-2. To a solution containing $Co(NO_3)_2{\cdot}6H_2O$ (60.0 mg, 0.21 mmol) in DMF (1.30 mL) added were terephthalic acid (49.8 mg, 0.30 mmol) and $TiCl_4(thf)_2$ (28.0 mg, 0.08 mmol). After it was stirred for about 30 min, the greenish solution was charged into a glass tube which was flame-sealed and heated stepwise to 70 °C (12 h), 90 °C (24 h) and then to 115 °C (72 h). The raw product obtained as microcrystals embeded in gel-like suspension was thoroughly washed with DMF. After solvent-exchange with CS_2, the product was dried under vacuum overnight (15 mg, 27%). Calcd for $Co_2Ti(O)(bdc)_3{\cdot}4H_2O$: C, 38.63; H, 2.70; N, 0.00; Co, 15.80; Ti, 6.42. Found: C, 38.70; H, 2.66; N, 0.00; Co, 16.02; Ti, 6.34%.

Received: June 14, 2013
Revised: July 29, 2013
Published: August 20, 2013

Gas Sorption Studies. BET gas sorption isotherms were measured with a Belsorp Mini-II at the following temperatures: liquid nitrogen (77 K), slush baths of dry ice-isopropylalcohol (195 K), ice–water (273 K), or warm water (298 K). The gases used were of the highest quality available (N60 for H_2 and N50 for CO_2, N_2 and N35 for CH_4). Approximately 100 mg of as-synthesized CTOFs were guest-exchanged with CH_2Cl_2 or CS_2 and evacuated under a dynamic vacuum (10^{-3} Torr) for 12 h. The equilibrium criteria were set consistent throughout all the measurements (change in adsorption amounts less than 0.1 cm^3/g within 180 s). The isosteric heats of CO_2 adsorption were calculated based on CO_2 adsorption at 273 and 298 K (SI Figure S3).

Powder X-ray Diffraction. Crystalline samples of CTOF-1 and CTOF-2 thoroughly ground in an agate mortar were packed in capillary tubes (0.3 mm diameter) with a few drops of DMF. The sample tubes were put into a custom-built housing that was connected to a vacuum pump and gas supply at the 2D SMC beamline of the Pohang Accelerator Laboratory, Korea. Debye–Scherrer diffraction data were collected on an ADSC Quantum-210 detector with a fixed wavelength (λ = 1.00000 Å) and an exposure of 60 s. After the first measurement at room temperature, the sample was gradually heated to 90 °C under reduced pressure until there was no change in the observed patterns. Then the tube was backfilled with CO_2 gas (800 Torr), and the temperature was lowered to 195 K before measuring diffractions, the sample was warmed to room temperature, and DMF was added into the tube before recording the final diffraction pattern. The temperatures were controlled by adjusting the stream of nitrogen gas (cooled or heated). The ADX program[4] was used for data collection, and Fit2D program[5] was used to convert the 2D to 1D patterns. Complete patterns are shown in SI Figure S4.

Single-Crystal X-ray Diffraction. Two different types of single-crystals for CTOF-1 were directly picked up from the mother liquor with a cryoloop attached to a goniohead, and transferred to a cold stream of liquid nitrogen (−173 °C). The data collection was carried out using synchrotron X-ray on a ADSC Quantum 210 CCD detector with a silicon (111) double-crystal monochromator at 2D SMC beamline of the Pohang Accelerator Laboratory, Korea. The ADSC Quantum-210 ADX program[4] was used for data collection, and HKL3000sm (version 703r)[6] was used for cell refinement, data integration, and absorption correction. After space group determination, the structures were solved by direct methods and subsequent difference Fourier techniques (SHEXLTL).[7] The ligand atoms including the hydroxyl group are found disordered and thus refined using split-atom models. Unlike CTOF-1w where disordered DMF molecules were found coordinated to the metal center, the structure of CTOF-1e did not show significant electron densities near coordinated solvent oxygen atoms. The metal site was refined assuming a simultaneous occupation by Co and Ti in a 2:1 ratio. All the non-hydrogen atoms were refined anisotropically, and hydrogen atoms were added to their geometrically ideal positions. The diffused electron densities resulting from residual solvent molecules could not be modeled properly, and therefore were removed from the reflection data using the SQUEEZE routine of PLATON.[8] The crystal data and results of structure refinements are summarized in SI Table S1. Disordered structures and the secondary building units are compared in SI Figure S5.

RESULTS AND DISCUSSION

CTOFs are synthesized as orange-brown crystals, when a mixture of cobalt(II) nitrate and titanium(IV) chloride tetrahydrofuran adduct reacts with 2-hydroxyterephthalic acid ($hbdcH_2$) or terephthalic acid ($bdcH_2$) in DMF. Note that neither Co(II) nor Ti(IV) alone does not produce any crystalline product with hbdc ligand under the same condition. The formula deduced from X-ray crystal structures is $[Co_2TiO(L)_3(solv)_3]$, where L is hbdc for CTOF-1 and bdc for CTOF-2. The structure of CTOF-1 is based on the so-called basic carboxylate units interconnected through hbdc dianions (Figure 1a).

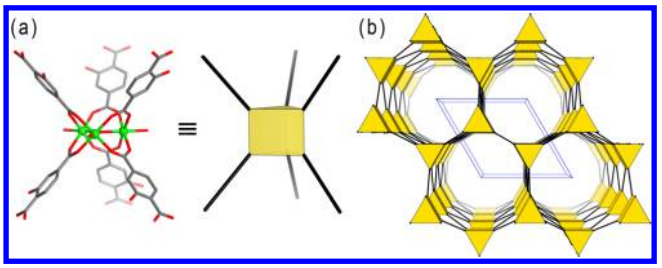

Figure 1. Geometry of the building block (a) and simplified network structure (b) of CTOF-1.

The trinuclear unit in CTOF-1 acts as a trigonal prism node and leads to the well-defined topology known as the **acs** net (Figure 1b).[9] The semiregular net having the transitivity of (1122) has been recognized, although not frequented, in MOFs with variations in the SBUs and linkers.[10]

The Co(II) and Ti(IV) ions are randomly distributed over the crystallographically equivalent metal sites, and the ratio of the two metal ions is established from the analysis of bulk samples using ICP-AES (67.0% Co and 33.0% Ti). CTOF-2 is obtained only as microcrystals not suitable for single crystal diffractions, and is isostructural with CTOF-1 judging from powder X-ray diffraction (PXRD) studies and other bulk analysis (see Experimental Section).

Interestingly, two different crystal habits are observed for CTOF-1 depending on the synthetic condition. When heated gradually to 115 °C over several days, large crystals (~0.5 mm) with double-pointed hexagonal block shape are obtained exclusively (Figures 2a). When heated rapidly to 150 °C, however, the same reaction produces a mixture with very small crystals (<0.1 mm) of hexagonal plate morphology (Figures 2b).

It turned out to our surprise that the two phases are essentially the same material with the identical connectivities according to synchrotron X-ray diffraction studies on single

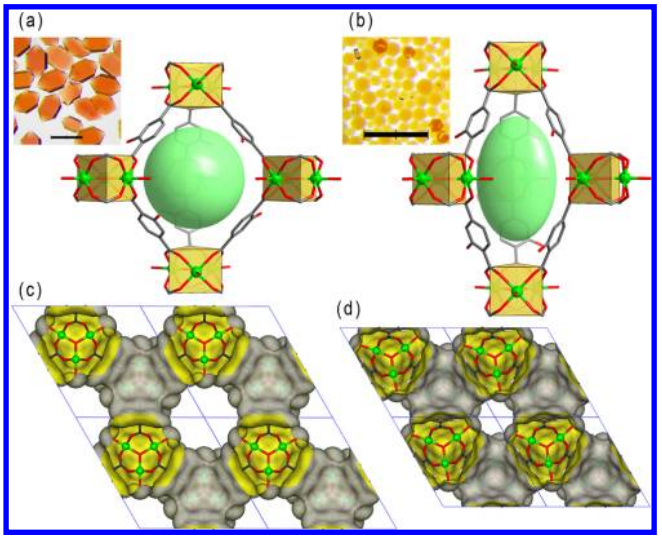

Figure 2. Photographs of the single crystals and X-ray structures for two polymorphs (CTOF-1w (a) and CTOF-1e (b)). The scale bar represents 0.5 mm length. Shown in panels c and d are the contact surfaces (1.4 Å) of the two structures drawn on a comparable scale.

dx.doi.org/10.1021/cg4009009 | Cryst. Growth Des. 2013, 13, 4066–4070

crystals. The two structures, however, possess different aspect ratio (c/a) in the hexagonal setting of the trigonal unit cells. We thus label the two as wide (w) and elongated (e) forms for convenience (Figure 2c and 2d).

The surprising bistability of CTOF-1 shown by the two independent crystal structures has prompted us to investigate their transformation. When subjected to PXRD, surface-dried samples of as-synthesized CTOF-1 and -2 displayed patterns inconsistent from measurements to measurements. Therefore, we packed finely ground samples along with a small amount of DMF inside capillary tubes, and measured Debye–Scherrer diffractions using synchrotron X-rays. The observed patterns showed good agreements with simulations based on the crystal structure of CTOF-1w (Figures 3 and 4).

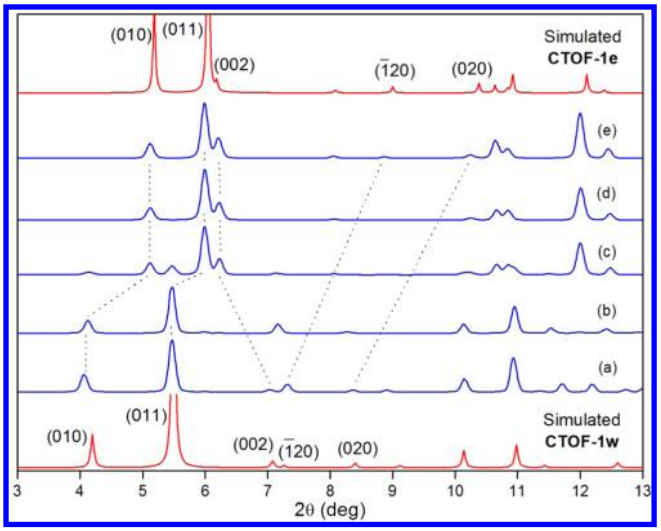

Figure 3. In situ PXRD patterns for CTOF-1 measured with synchrotron X-rays (λ = 1.0000 Å). (a) As-synthesized, (b–d) heated to 90 °C under reduced pressures, and (e) backfilled with DMF.

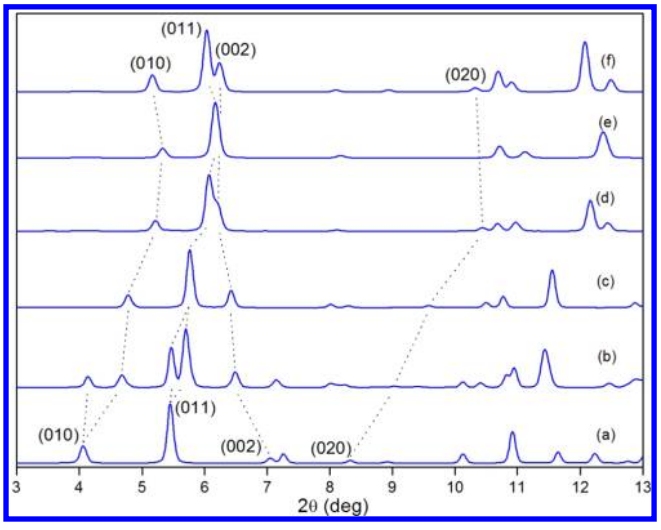

Figure 4. In situ PXRD patterns for CTOF-2 measured with synchrotron X-rays (λ = 1.0000 Å). (a) As-synthesized, (b–d) heated to 90 °C under reduced pressures, (e) backfilled with 1 bar CO_2 at 195 K, and (f) backfilled with DMF at room temperature.

Subsequently, in situ diffraction patterns were recorded while the wet samples were heated under reduced pressures. As expected, dramatic changes have been observed in which most of the peaks except for (00l) shifted to higher angles, while (002) reflection moves to lower angle because of the elongation along the *c* axis. Overall, the changes are very similar for CTOF-1 and 2, and the final diffraction patterns corroborate with the simulation from the crystal structure of CTOF-1e. The structural changes occur quite fast and complete within 20–30 min upon departure; however, additional change from the elongated form has not been observed even after heating the samples overnight under vacuum (SI Figure S4). Furthermore, the transition could not be reversed to the wide form by filling the evacuated samples with CO_2 (195 K), air, or DMF solvent (298 K), implying the higher stability of the more compact elongated form.[11]

Structurally flexible MOFs often show reversible breathing behavior associated with the degree of solvation and conformational changes of organic ligands.[12] The transition between the two polymorphs of CTOF-1 does not involve such structural changes and is irreversible upon resolvation with DMF.[13] It is also interesting that despite the similarity of their structures, the dynamic behavior of CTOF-1 is fundamentally different from the series of MIL-88,[10b] for which the as-synthesized form is an intermediate phase between two extremes of expanded and constricted forms.[14]

The network structure of CTOF-1e is featured with ellipsoidal pores (6–9 Å) interconnected through straight channels (~6 Å). According to thermogravimetric analysis, the solvent molecules occupying these voids as well as those coordinated to metal centers are removed in two well-separated steps, and the frameworks does not decompose before 300 °C (SI Figure S1).

Once void of guest solvent molecules in the pores, CTOF-1 and 2 can reversibly adsorb N_2, CO_2, H_2, and CH_4 (Figure 5). Note that for both CTOFs the elongated form represents the porous phase as unambiguously shown by PXRD. The saturated adsorptions for N_2 (77 K) and CO_2 (195 K) are similar for the two CTOFs, resulting in the BET (Langmuir) surface areas of 637 (751) and 618 (726) m^2/g for CTOF-1 and CTOF-2, respectively. Interestingly, the uptake capacities measured at 1 bar pressure of H_2 (77 K) and CH_4 (195 K) show large differences with the values for CTOF-2 being 39–106% higher than those of CTOF-1. It is believed that the presence of hydroxyl groups around pores in CTOF-1 delimit the free passage causing hindered diffusions for adsorbates in the channels. For CO_2 at higher temperatures, the relatively polar surface of CTOF-1 may be preferred because of the interaction with the quadrupolar moment, resulting in higher uptake and isosteric heats of adsorption, which are in the range 28–32 kJ/mol (SI Figure S3).

Previously known MOFs closely related to CTOFs in terms of the building blocks and topology include those of Sc^{3+},[15] Cr^{3+} (MIL-88B),[10b] or Fe^{3+} (MOF-235);[9b] however, none of these has been reported with a proof of permanent porosity. This is partly because MOFs based on $M_3O(CO_2)_6$ units often suffer from unbalanced charges when interconnected through dicarboxylate linkers, and the presence of counterions significantly reduces pores available for guest uptake. Rational approaches to obtain charge-neutral frameworks should therefore rely on either homonuclear mixed-valence or heterovalent-mixed-metal systems.[16] Contrary to the limited cases of mixed-valence approach, the latter method can be readily employed by varying chemical compositions during the synthesis, as in the case of CTOFs. In addition to the X-ray structures and the established Co/Ti ratio, the absence of

dx.doi.org/10.1021/cg4009009 | *Cryst. Growth Des.* 2013, 13, 4066–4070

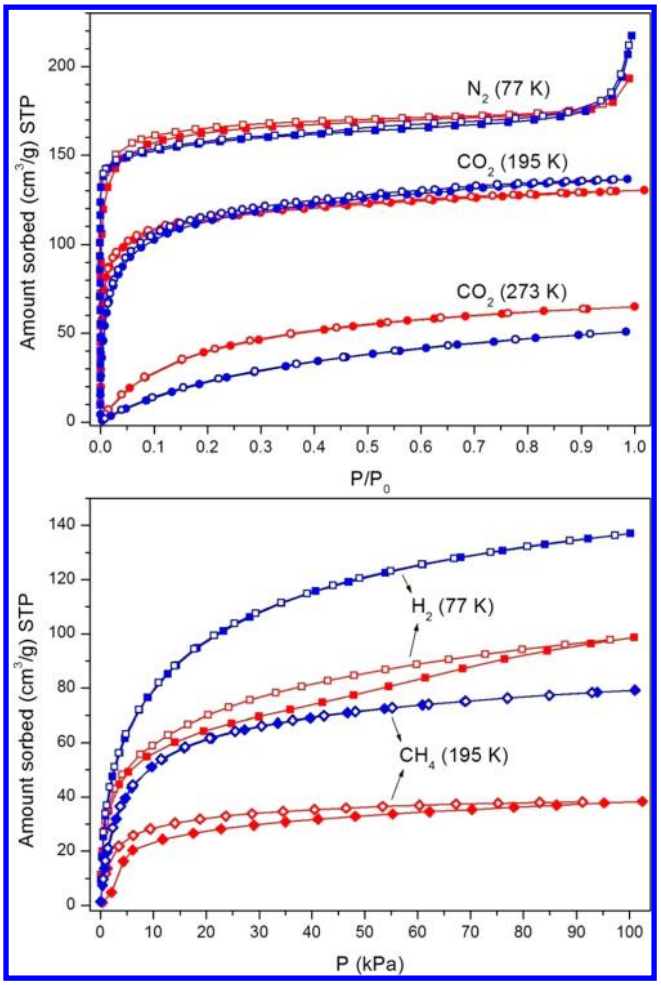

Figure 5. Gas sorption isotherms for CTOF-1 (red) and CTOF-2 (blue). Filled and open symbols represent adsorption and desorption, respectively.

nitrogen in the evacuated solids is another evidence that the frameworks of CTOF-1 and CTOF-2 are indeed void of counterions, such as dimethylammonium or nitrate (see Experimental Section). FT-IR spectroscopy also confirms the absence of such species (SI Figure S2).

In conclusion, the cobalt−titanium-organic frameworks synthesized in this work are not simple variations of their homonuclear analogues, but display unique properties, such as a bistability and irreversible phase transitions. The M(II)−M′(IV) heterometallic approach is also beneficial in endowing a permanent porosity to MOFs based on building blocks with intrinsically unbalanced charges. Systematic investigations with other combination of metals may lead to new MOFs with even more interesting properties.

■ ASSOCIATED CONTENT

Supporting Information

Details of the synthesis and X-ray crystal structure analysis and IR, TGA, gas sorption, and PXRD data. This material is available free of charge via the Internet at http://pubs.acs.org.

■ AUTHOR INFORMATION

Corresponding Author

*Phone: +82-31-400-5506. Fax: +82-31-400-5457. E-mail: (H.C.) hchun@hanyang.ac.kr. E-mail: (D.M.) dmoon@postech.ac.kr.

Notes

The authors declare no competing financial interest.

■ ACKNOWLEDGMENTS

This work was supported by the National Research Foundation of Korea Grant funded by the Korean Government (013-2011-1-C00039), and the Basic Science Research Program of NRF Korea (2012R1A1A2004333). H.C. thanks DND (Novosibirsk, Russia) for helpful discussions.

■ REFERENCES

(1) (a) Zhang, Z.; Zhao, Y.; Gong, Q.; Li, Z.; Li, J. *Chem. Commun.* **2013**, *49*, 653. (b) Dhakshinamoorthy, A.; Alvaro, M.; Garcia, H. *Chem. Commun.* **2012**, *48*, 11275. (c) Bae, Y.-S.; Snurr, R. Q. *Angew. Chem., Int. Ed.* **2011**, *50*, 11586. (d) Allendorf, M. D.; Schwartzberg, A.; Stavila, V.; Talin, A. A. *Chem.—Eur. J.* **2011**, *17*, 11372. (e) D'Alessandro, D. M.; Smit, B.; Long, J. R. *Angew. Chem., Int. Ed.* **2010**, *49*, 6058. (f) McKinlay, A. C.; Morris, R. E.; Horcajada, P.; Férey, G.; Gref, R.; Couvreur, P.; Serre, C. *Angew. Chem., Int. Ed.* **2010**, *49*, 6260. (g) Horike, S.; Shimomura, S.; Kitagawa, S. *Nat. Chem.* **2009**, *1*, 695. (h) Lee, J. Y.; Farha, O. K.; Roberts, J.; Scheidt, K. A.; Nguyen, S. T.; Hupp, J. T. *Chem. Soc. Rev.* **2009**, *38*, 1450. (i) Czaja, A. U.; Trukhan, N.; Müller, U. *Chem. Soc. Rev.* **2009**, *38*, 1284. (j) Kuppler, R. J.; Timmons, D. J.; Fang, Q.-R.; Li, J.-R.; Makal, T. A.; Young, M. D.; Yuan, D.; Zhao, D.; Zhuang, W.; Zhou, H.-C. *Coord. Chem. Rev.* **2009**, *253*, 3042.

(2) (a) Frigoli, M.; El Osta, R.; Marrot, J.; Medina, M. E.; Walton, R. I.; Millange, F. *Eur. J. Inorg. Chem.* **2013**, 1138. (b) Kozachuk, O.; Khaletskaya, K.; Halbherr, M.; Bétard, A.; Meilikhov, M.; Seidel, R.; Jee, B.; Pöppl, A.; Fischer, R. *Eur. J. Inorg. Chem.* **2012**, 1688. (c) Nouar, F.; Devic, T.; Chevreau, H.; Guillou, N.; Gibson, E.; Clet, G.; Daturi, M.; Vimont, A.; Grenéche, J. M.; Breeze, M. I.; Walton, R. I.; Llewellyn, P. L.; Serre, C. *Chem. Commun.* **2012**, *48*, 10237. (d) Zheng, S.-T.; Wu, T.; Chou, C.; Fuhr, A.; Feng, P.; Bu, X. *J. Am. Chem. Soc.* **2012**, *134*, 4517. (e) Das, M. C.; Xiang, S.; Zhang, Z.; Chen, B. *Angew. Chem., Int. Ed.* **2011**, *50*, 10510. (f) Nayak, S.; Harms, K.; Dehnen, S. *Inorg. Chem.* **2011**, *50*, 2714. (g) Zou, R.; Zhong, R.; Han, S.; Xu, H.; Burrell, A. K.; Henson, N.; Cape, J. L.; Hickmott, D. D.; Timofeeva, T. V.; Larson, T. E.; Zhao, Y. *J. Am. Chem. Soc.* **2010**, *132*, 17996.

(3) Hong, K.; Bak, W.; Chun, H. *Inorg. Chem.* **2013**, *52*, 5645.

(4) Arvai, A. J.; Nielsen, C. *ADSC Quantum-210 ADX Program*; Area Detector System Corporation; Poway, CA, U.S.A., 1983.

(5) Hammersley, A. *Fit2D Program*; ESRF: Grenoble, France, 2004.

(6) Otwinowski, Z.; Minor, W. *Methods in Enzymology*; Carter, C. W., Jr., Sweet, R. M., Eds.; Academic Press: New York, 1997; Vol. *276*, part A, p 307.

(7) Sheldrick, G. M. *SHELXTL-PLUS, Crystal Structure Analysis Package*; Bruker Analytical X-Ray; Madison, WI, U.S.A., 1997.

(8) Spek, A. L. *PLATON, A Multipurpose Crystallographic Tool*; Utrecht University: Utrecht, the Netherlands, 2001.

(9) (a) Friedrichs, O. D.; O'Keeffe, M.; Yaghi, O. M. *Acta Crystallogr., Sect. A* **2003**, *59*, 515. (b) Sudik, A. C.; Côté, A. P.; Yaghi, O. M. *Inorg. Chem.* **2005**, *44*, 2998.

(10) (a) Jeong, S.; Song, X.; Jeong, S.; Oh, M.; Liu, X.; Kim, D.; Moon, D.; Lah, M. S. *Inorg. Chem.* **2011**, *50*, 12133. (b) Serre, C.; Mellot-Draznieks, C.; Surble, S.; Audebrand, N.; Filinchuk, Y.; Férey, G. *Science* **2007**, *315*, 1828. (c) Wang, Z.; Zhang, B.; Inoue, K.; Fujiwara, H.; Otsuka, T.; Kobayashi, H.; Kurmoo, M. *Inorg. Chem.* **2007**, *46*, 437. (d) Devic, T.; Serre, C.; Audebrand, N.; Marrot, J.; Férey, G. *J. Am. Chem. Soc.* **2005**, *127*, 12788. (e) Yang, G.; Raptis, R. G. *Chem. Commun.* **2004**, 2058.

(11) The unit cell volume of CTOF-1e is 75% that of CTOF-1w.
(12) (a) Horike, S.; Shimomura, S.; Kitagawa, S. *Nat. Chem.* **2009**, *1*, 695. (b) Férey, G.; Serre, C. *Chem. Soc. Rev.* **2009**, *38*, 1380. (c) Gagnon, K. J.; Beavers, C. M.; Clearfield, A. *J. Am. Chem. Soc.* **2013**, *135*, 1252. (d) Salles, F.; Maurin, G.; Serre, C.; Llewellyn, P. L.; Knöfel, C.; Choi, H. J.; Filinchuk, Y.; Oliviero, L.; Vimont, A.; Long, J. R.; Férey, G. *J. Am. Chem. Soc.* **2010**, *132*, 13782.
(13) We do not rule out the possibility of a reversible transition under a condition that has not been examined in this work.
(14) The resistance of a mixed-valence MOF toward breathing effects has been reported. See Liu, Y.-Y.; Couck, S.; Vandichel, M.; Grzywa, M.; Leus, K.; Biswas, S.; Volmer, D.; Gascon, J.; Kapteijn, F.; Denayer, J. F. M.; Waroquier, M.; Van Speybroeck, V.; Van Der Voort, P. *Inorg. Chem.* **2013**, *52*, 113.
(15) Dietzel, P. D. C.; Blom, R.; Fjelvåg, H. *Dalton Trans.* **2006**, 2055.
(16) For mixed-metal basic carboxylate clusters, see Tranchemontagne, D. J.; Mendoza-Cortés, J. L.; O'Keeffe, M.; Yaghi, O. M. *Chem. Soc. Rev.* **2009**, *38*, 1257.